

Performance Analysis of LLC-LC Resonant Converter Fed PMDC Motor

M. Santhosh Rani and Subhransu Sekhar Dash

SRM University, Chennai, India
brsr68@gmail.com, munu_dash_2k@yahoo.com

Abstract

In this paper, a modified form of the most efficient resonant LLC series parallel converter configuration (SPRC) is proposed. The proposed system comprises of an additional LC circuit synchronized along with the existing resonant tank of LLC configuration (LLC-LC configuration). With the development of power electronics devices, resonant converters have been proved to be more efficient than conventional converters as they employ soft switching technique. Among the three basic configurations of resonant converter, Series Resonant Converter (SRC), Parallel Resonant Converter (PRC) and Series Parallel Resonant Converter, the LLC configuration under SPRC is proved to be most efficient providing narrow switching frequency range for wide range of load variation, improved efficiency and providing ZVS capability even at no load. The modified LLC configuration i.e., LLC-LC configuration offers better efficiency as well as better output voltage and gain. The efficiency tends to increase with increase in input voltage and hence these are suitable for high input voltage operation. In this paper, LLC topology of SPRC and a modified LLC topology (LLC-LC) of SPRC for the closed loop control of a BLDC motor are simulated and their performances are compared and analyzed.

Keywords: LLC converter, LLC-LC converter, PMDC motor, Full-bridge converter, Soft switching converter, Series-Parallel resonant converter.

1. Introduction

Resonant converters are DC-DC switching converters that include resonant tank circuit actively participating in determining input to output power flow. Resonant DC-DC converters are preferred over other conventional topologies due to its features like soft switching namely ZVS and ZCS[1], high frequency operation, high efficiency, smaller size, light weight, low component stress and reduced EM interference. Several topologies of resonant converters have been designed and tested which can all be grouped in the form of one building block as resonant inverter. The block diagram of resonant converter is shown in Figure 1. The resonant DC-DC converter basically comprises of three main building blocks namely Resonant Inverter, rectifier and a Low pass filter.

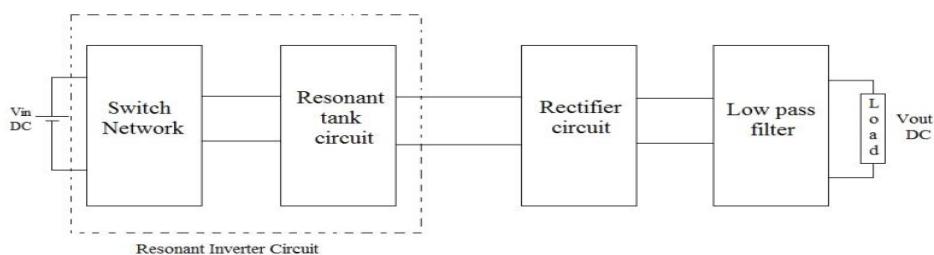


Figure 1. Block Diagram of Resonant DC-DC Converter

The switch network can be half bridge or full bridge [2],[3] designed with various power electronics switches. The second sub block of resonant inverter is resonant tank circuit. It comprises of inductance and capacitor arranged in different configurations. Among all the possible configurations, three main topologies namely Series Resonant Converter (SRC), Parallel Resonant Converter (PRC) and Series Parallel Resonant Converter (SPRC) are widely used for different applications.

In SRC shown in Figure 2. the resonant inductor and capacitor are in series and the load is arranged in series with the resonant tank circuit. This operates quite efficiently in the ZVS region, for switching frequency greater than resonant frequency but fails to operate in ZCS region where switching frequency becomes less than resonant frequency, thus giving rise to problems such as light load regulation, high circulating energy and high turn off current at high input voltage conditions. Light load regulation can be overcome with additional control techniques.

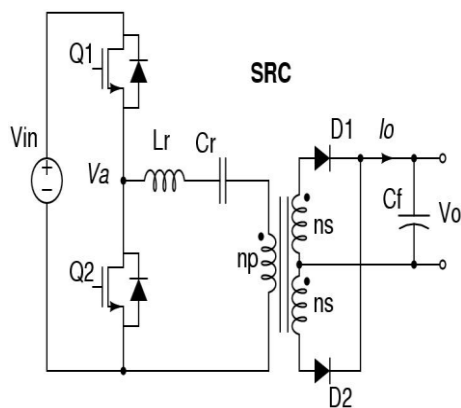


Figure 2. Half Bridge LLC SPRC

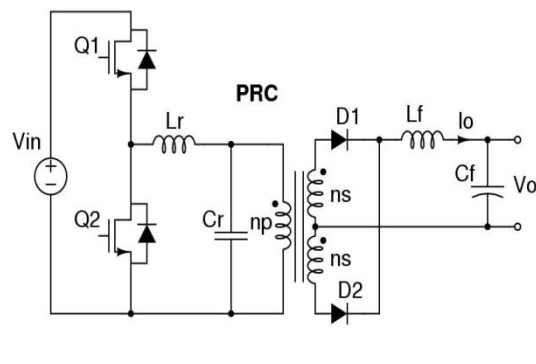


Figure 3. Half Bridge LCC SPRC

In PRC shown in Figure 3, load is connected in parallel to the resonant capacitor which is actually connected in series with the resonant inductor. Light load regulation problem of SRC is overcome in PRC but the circulating energy increases more than that of SRC. Also, the turn off current is high at high input voltage thus increasing losses.

In SPRC which is a combination of SRC and PRC, an inductive or capacitive element is connected in series with a series combination of resonant inductor and capacitor. The load is connected in parallel to this third element. Based on the third element, two configurations are possible as LCC & LLC. SPRC is formed to get the better qualities of both SRC and PRC. In LCC configuration of SPRC shown in Figure 4, high conduction and switching losses occur. Moreover it operates in ZCS region further increasing the loss and decreasing efficiency. On the other hand, LLC [4]-[6] as shown in Figure 5, is considered to be the best among the above mentioned converters due to its advantages like ZVS capability even at no load condition and the narrow switching frequency range with light load.

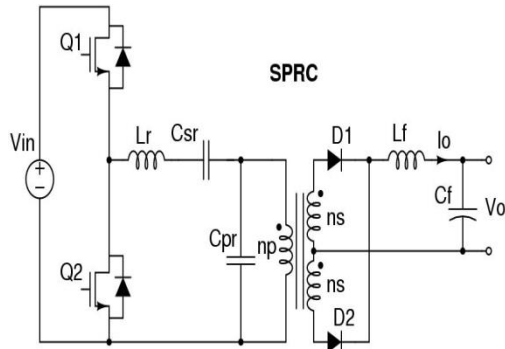


Figure 4. Half Bridge LCC Series Parallel Converter

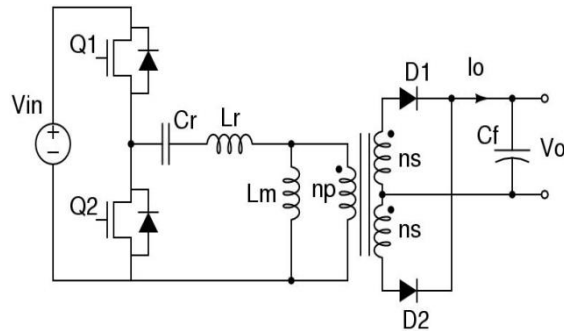


Figure 5. Half Bridge LLC Series Parallel Converter

Equivalent circuit of LLC [7] and closed loop control by controlling the switches with reference to output voltage is carried out in [8]. By splitting the secondary side of the transformer before the rectifier circuit, how two outputs can be obtained at the same time is dealt in [8]. Also how solar array simulator use LLC converter for its input voltage is discussed and the transfer function is derived in [10]. Optimization of LLC converter's performance using a mode solver technique is discussed in [11]. By introducing an extra LC circuit in the resonant tank, a new modified form of LLC converter is implemented in [12].

BLDC motor is considered to be better than other motors due to its brushless nature. Also electronic commutation can be carried out for both sensor motor [13] and sensorless BLDC motor [14] which makes the system cheap and the speed is controlled using field oriented control [15].

2. LLC Resonant Converter

The LLC topology of resonant converter has resonant tank of an inductor (L_r) in series with capacitor (C_r) which are then connected to one more inductor (L_m) across which the load is arranged in parallel. The resonant tank of the LLC topology is as shown in Figure 6.

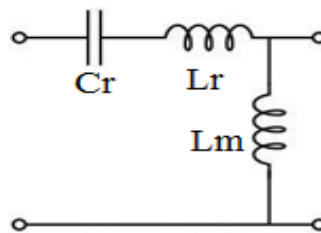


Figure 6. Resonant Tank of LLC Converter

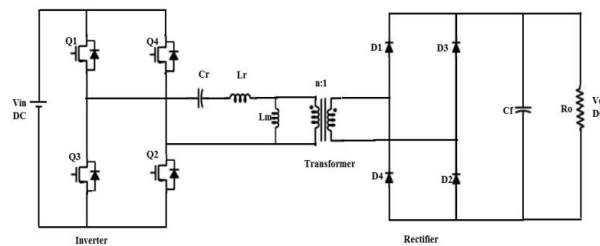


Figure 7. Full Bridge Configuration of LLC Converter

Due the introduction of third extra element L_m , two resonant frequencies are obtained, one due to the series combination of L_r & C_r and second one due to the series combination of $(L_r + L_m)$ & C_r . The lower frequency usually falls in the ZCS region and hence it cannot be designed to operate at this region. The frequencies are given by equations (1) and(2). Full bridge configuration of LLC converter is shown in Figure 7.

$$f_{r1} = \frac{1}{2\pi\sqrt{L_r C_r}} \quad (1)$$

$$f_{r2} = \frac{1}{2\pi\sqrt{(L_r + L_m) C_r}} \quad (2)$$

2.1. Operation of LLC Converter

The DC characteristic of LLC resonant converter is shown in Figure 8. The characteristic is subdivided into ZVS region and ZCS region. On the right side of f_{r1} , this converter has same characteristic of SRC. On the left side of f_{r1} , the feature of PRC and SRC are fighting to be the dominant. At heavy load, SRC feature is dominant. When load gets lighter, characteristic of PRC is dominant. Depending on the modes of operation, the same characteristics can be subdivided into three as region 1, region 2 and region 3 as shown in Figure 9.

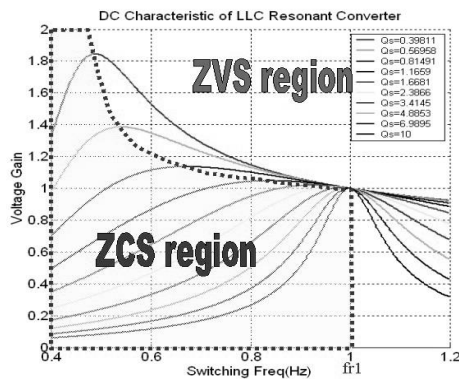


Figure 8. DC Characteristics of LLC Converter

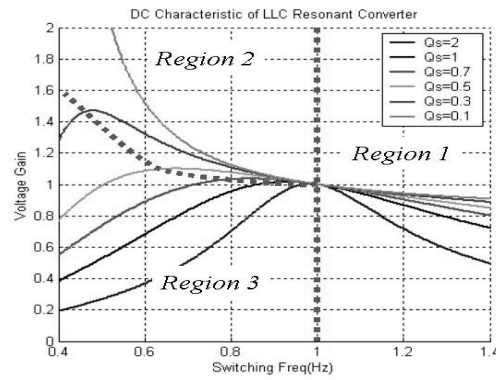


Figure 9. Three Operating Regions of LLC Converter

In region 1, the converter works very similar to SRC. In this region, L_m never resonates with resonant capacitor C_r . It is clamped by output voltage and acts as the load of the series resonant tank. With this passive load, LLC resonant converter is able to operate at no load condition without the penalty of very high switching frequency. Also, with passive load L_m , ZVS could be ensured for any load condition.

In region 2, the operation of LLC resonant converter is more complex and interesting. The waveforms could be divided into clearly two time intervals. In first time interval, L_r resonant with C_r . L_m is clamped by output voltage. When L_r current resonant back to same level as L_m current, the resonance of L_r and C_r is stopped, instead, now L_m will participate into the resonance and the second time interval begins. During this time interval, the resonant components will change to C_r and L_m in series with L_r . In fact, that is a part of the resonant process between $(L_m + L_r)$ with C_r . From this aspect, LLC resonant converter is a multi-resonant converter since the resonant frequency at different time interval is different. Because of the resonance between L_m and C_r , a peak on the gain appears at resonant frequency of $(L_m + L_r)$ and C_r .

In region 3, the impedance of resonant tank is capacitive, hence primary switches operate under ZCS condition, but the current spike during turn on transient will result in

high current stress and high switching loss. Hence, it should be prevented from operating in this region.

The equivalent circuit of LLC converter can be shown as in Figure 10. V_{ab} is the ac voltage generated from the inverter circuit of the resonant converter which is then supplied to the resonant tank. The load on the secondary side of the transformer is taken to be equivalent referred to the primary side of the transformer and indicated using R_i across which the output DC voltage is obtained.

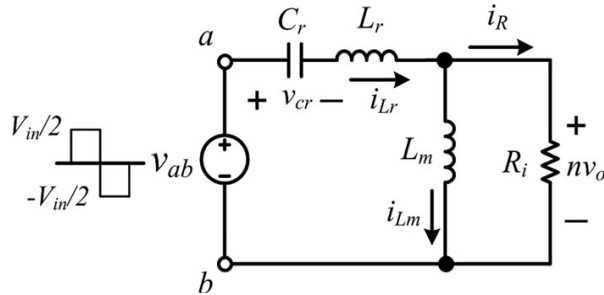


Figure 10. Equivalent Circuit of LLC Converter

Taking A as resonant inductance ratio (3), second resonant frequency ω_{r2} as ω_L and load quality factor, Q_L (4), we have,

$$A = \frac{L_r}{L_m} \quad (3)$$

$$Q_L = R_i \cdot \sqrt{\frac{C_r}{L_r + L_m}} \quad (4)$$

Taking Kirchoff's voltage equation, across 1st loop, we get,

$$V_{ab} = i \cdot (X_{C_r} + X_{L_r} + X_{L_m}) - i_R \cdot X_{L_m} \quad (5)$$

$$i_R = \frac{i \cdot X_{L_m}}{(R_i + X_{L_m})} \quad (6)$$

$$i_R = \frac{n \cdot V_o}{R_i} \quad (7)$$

On equating (6) & (7), we get,

$$i = \frac{n \cdot V_o \cdot (R_i + X_{L_m})}{R_i \cdot X_{L_m}} \quad (8)$$

On substituting (7) & (8) in (5), and solving we find the transfer function of LLC converter given as in (9);

$$\left| \frac{V_o}{V_i} \right| = \frac{1}{2n \cdot \sqrt{(1+A)^2 \cdot \left(1 - \left(\frac{\omega L}{\omega}\right)^2\right)^2 + \left(\frac{1}{Q_L}\right)^2 \cdot \left(\frac{\omega}{\omega_L}\right) \left(\frac{A}{1+A}\right) - \left(\frac{\omega L}{\omega}\right)^2}} \quad (9)$$

3. Modified LLC: LLC-LC Resonant Converter

LLC topology can be made more efficient by introducing extra LC components in the circuit. The LLC resonant converter has been widely used as a constant output voltage SMPS. LLC resonant converter can handle a widely adjustable regulated output voltage (or current) by using frequency control, even when wide input voltage or output load variations are applied to the converter. In this converter, large inductance ratio and wide switching frequency variations are required to achieve wide output adjustment range and to cover wide input voltage and load changes. High peak voltage is applied to the resonant capacitor, too. These problems limit the output adjustable range. Also, there is high-frequency ringing at the rectifying stage of the LLC resonant converter. These problems are eliminated in the modified LLC-LC topology.

At the rectifier stage, diodes are turned on and off at zero voltage condition instead of zero current condition which occurs in LLC resonant converter. Thus, the switching losses and noises due to reverse recovery process are reduced, making LLC-LC a better choice for high switching frequency operation. The full bridge configuration for LLC-LC is shown in Figure 11.

3.1. Design of LLC-LC Converter

In the LLC-LC topology, series combination of inductor (L_s) & capacitor (C_s) is introduced in series with the resonant tank of the LLC circuit on the secondary side of the transformer before the rectification stage of the converter.

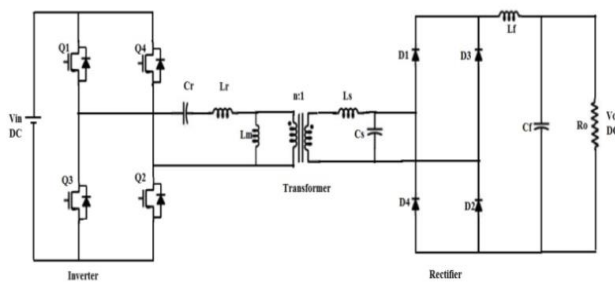


Figure 11. Full Bridge Configuration of LLC-LC Converter

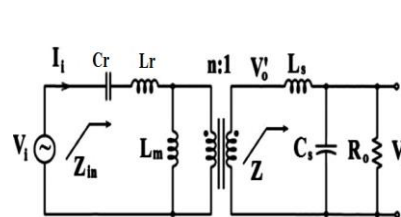


Figure 12. Equivalent Circuit of LLC-LC resonant Converter

The equivalent circuit for the LLC-LC converter is as shown in Figure 12. The input voltage, V_i is the equivalent DC voltage applied in the initial stage. The primary side of transformer shows the same primary of that of equivalent of LLC converter but the secondary side of the converter has equivalent load of rectification stage with the load in series with the inductor and capacitor combination of secondary side. The transfer function or the voltage gain for the LLC-LC topology is obtained as (10).

$$\frac{V_o}{V_i} = \frac{n \cdot A_p \cdot R_n \cdot f_n^2}{R_n \cdot X + j \cdot Y} \quad (10)$$

Where, the normalized frequency f_n , resonant frequency f_r , AC equivalent circuit normalized load resistance R_n , converter capacitance ratio A_c , primary inductance ratio A_p , secondary inductance ratio A_s and variables X and Y are given in Equations (11 to 18)

$$f_n = \frac{f_s}{f_r} \quad (11)$$

$$f_r = \frac{1}{2\pi\sqrt{L_r \cdot C_r}} \quad (12)$$

$$R_n = \frac{R_0}{\sqrt{L_r / C_r}} \quad (13)$$

$$A_c = \frac{C_s}{C_p} \quad (14)$$

$$A_p = \frac{L_r}{L_m} \quad (15)$$

$$A_s = \frac{L_s}{L_m} \quad (16)$$

$$X = n^2 [A_p \cdot (f_n^2 - 1) + f_n^2] (A_p - A_c \cdot A_s \cdot f_n^2) + (A_c \cdot A_p \cdot f_n^2 (1 - f_n^2)) \quad (17)$$

$$y = f_n \cdot [n^2 \cdot A_s (A_p (f_n^2 - 1) + f_n^2) + A_p (f_n^2 - 1)] \quad (18)$$

4. Closed Loop Control of BLDC

Brushless DC Motor (BLDC) is a type of synchronous motor used in industries like electronic appliances, automation, aerospace, consumer & medical fields due to several advantages like support to electronic commutation, Less maintenance due to less number of brushes, longer life, better heat dissipation, Higher speed range as no brushes limit its mechanical moment, better efficiency, flat speed and torque characteristics and no experience of slip.

In BLDC, the magnetic field generated by the stator and the magnetic field generated by the rotor rotates at same frequency. BLDC motors corresponding to the number of stator windings are categorized as 1phase, 2phase or 3phase. The stator windings can be either trapezoidal or sinusoidal, depending on the interconnection of coils in the stator windings to give different types of back electromotive force. Rotors are made up of permanent magnets and vary from two to eight pole pairs with alternate north and south poles.

The operation of a three phase BLDC motor is considered here for sinusoidal back EMF. The input supply is provided with the help of resonant converter. The resonant converter yields a DC output voltage which is then transformed to 3 phase AC voltage using an inverter which in turn runs the motor. The speed control is carried out in two ways either open loop control or closed loop control. The block diagram for open loop speed control of BLDC motor fed from resonant converter is as shown in Figure 13.

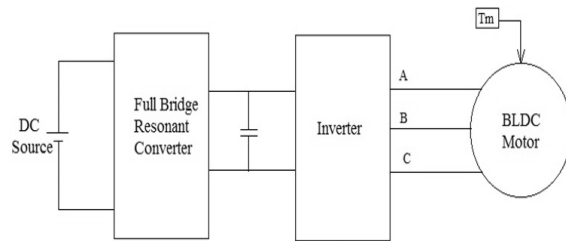


Figure 13. Block Diagram of BLDC Fed from Resonant Converter

The closed loop control uses the parameters of motor and compares it with a preset value and control circuit is applied at the inverter level.

BLDC motor has an advantage of being able to be electronically commutated. This is effective for sensed motor where the commutation is carried out by sensing the position of rotor and as per that commutation is applied. But it is not always possible as speed sensors are objectionable for use in explosive environment such as chemical industries. In order to reduce the cost and to increase the mechanical robustness of the system, it is advisable to avoid using sensors. Hence closed loop speed control of sensorless BLDC motor using field oriented control technique is considered in this work.

4.1. Field Oriented Control

The closed loop control is carried out using field oriented control approach. Field Oriented Control is based on the machine current and voltage space vectors, the transformation of a three phase speed and time dependent system into a two co-ordinate time invariant system and effective Pulse Width Modulation pattern generation.

Field oriented controlled machines need two constants as input references: the torque component (aligned with the q co-ordinate) and the flux component (aligned with d co-ordinate). As Field Oriented Control is simply based on projections, the control structure handles instantaneous electrical quantities. This makes the control accurate in every working operation (steady state and transient) and independent of the limited bandwidth mathematical model. Block diagram of field oriented control is shown in Figure 14.

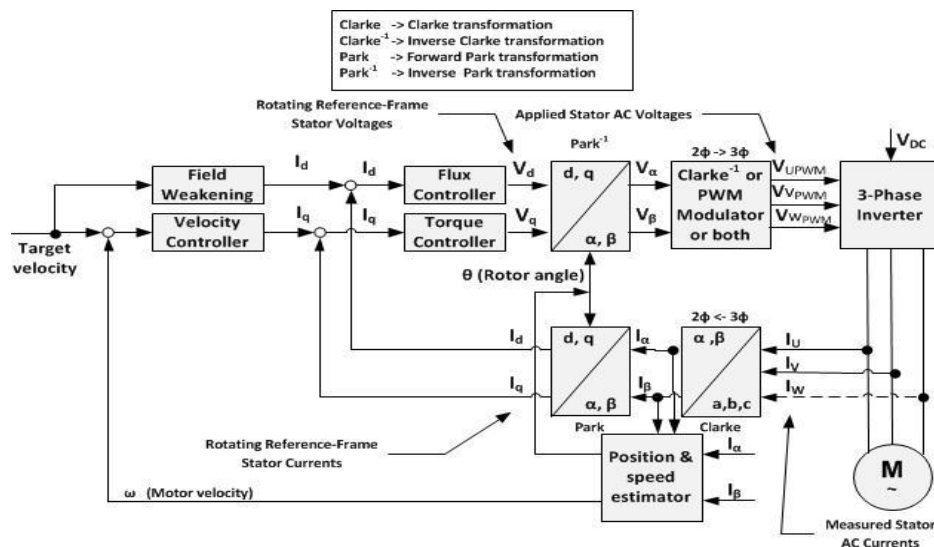


Figure 14. Block Diagram of Field Oriented Control

The main functioning of field control lies in the manipulation of motor currents and voltages. The input current of the motors are converted from their three axis reference frame to a two axis frame and then again that two axis orthogonal frame is converted to two axis rotating frame. These signals generated undergo the control device, as PI controller and then generate the voltage in two axis frame after undergoing integration. The generated two axis voltages are transformed back to two axis stationary states which are again transformed to three axis configurations. These voltages undergo pulse modulation and then are applied as the controlling pulses for the three phase inverter stage. Thus, the closed loop control using field oriented control is carried out. The field oriented control is summarized in six steps namely as follows;

4.1.1. Clarke Transformation: The first step referred as Clarke transform, converts a rotating three axis frame to stationary orthogonal two axis frame; i.e., from a-b-c frame to α - β frame using the equations as follows;

$$i_a + i_b + i_c = 0 \quad (19)$$

$$i_\alpha = i_a \quad (20)$$

$$i_\beta = \frac{1}{\sqrt{3}} \cdot i_a + \frac{2}{\sqrt{3}} \cdot i_b \quad (21)$$

4.1.2. Park Transformation: The second step referred as Park transform, converts a two axis orthogonal system to a rotating two axis system; i.e., from α - β frame to d-q frame using the equations as follows;

$$i_d = i_\alpha \cdot \cos \theta + i_\beta \cdot \sin \theta \quad (22)$$

$$i_q = -i_\alpha \cdot \sin \theta + i_\beta \cdot \cos \theta \quad (23)$$

4.1.3. PID Controller: A PID controller actually responds to an error signal generated by calculating the difference between the signal generated and a reference value. The controller responds to this error signal and adjusts the controlled quantity to achieve the desired response by changing few gain values. The sign of the error indicates the direction of change in the control signal. P represents proportional part which is obtained by multiplying the error signal by a gain, causing the controller to produce a response that is a function of the error signal. 'I' represents integral part which is used to eliminate small steady state errors. 'I' term calculates a continuous running total of the error signal. Hence, a small steady state error accumulates into a large error value over time. This accumulated error signal is multiplied by an 'I' gain factor and becomes the 'I' output term of the PID controller represents differential term which is used to enhance the speed of the controller and responds to the rate of change of error signal. Here only PI terms are used to avoid the slow response time of motor speed change.

The P gain of the controller sets the overall system response. When controller is tuned initially, I and D are set to zero. Then the P gain is increased until the system responds to set point changes without excessive overshoot or oscillations. Using lower values of 'P' gain will loosely control the system, while higher values will give stiff values. At this point, the system will probably not converge to the set point. After this, 'I' gain can be increased so as to force the system error to zero. A slight increase is sufficient in 'I' such that it does not overcome the effects of 'P' gain.

4.1.4. Inverse Park Transformation: After PI control, two voltage signals are obtained in rotating frame. Hence, Inverse Park transform is used to now obtain those in orthogonal frame, i.e., converting voltage from d-q frame to α - β frame by using following equations;

$$i_\alpha = i_d \cdot \cos \theta - i_q \cdot \sin \theta \quad (24)$$

$$i_{\beta} = i_d \cdot \sin \theta + i_q \cdot \cos \theta \quad (25)$$

4.1.5. Inverse Clarke Transformation: The next step referred as Inverse Clarke transform is used to convert α - β frame to a-b-c frame, i.e., two orthogonal axis system is converted to three axis system with the help of following equations;

$$i_a = i_{\alpha} \quad (26)$$

$$i_b = -\frac{1}{2} \cdot i_{\alpha} + \frac{\sqrt{3}}{2} \cdot i_{\beta} \quad (27)$$

$$i_c = -\frac{1}{2} \cdot i_{\alpha} - \frac{\sqrt{3}}{2} \cdot i_{\beta} \quad (28)$$

4.1.6 Pulse Width Modulation: Six pulses required for the operation of the switching circuit of the inverter are generated by comparing three sinusoidal output voltage waveforms generated after Inverse Park transformation, i.e., voltages of a-b-c frame with respect to triangular repeating sequence.

5. Resonant Converter fed BLDC Motor- Simulation & Results

MATLAB is chosen as the environment for simulating and analyzing the performance of the conventional and modified form of the LLC Resonant Converter and then the speed control of BLDC motor is also carried out in Simulink environment and their outputs are compared.

5.1. LLC Resonant Converter

The resonant converter's operation depends on the inductance ratio (A), transformer turns ratio (n), resonant inductor and capacitor. Keeping the transformer turns ratio constant, nine different cases of operation are possible depending on the relation between switching frequency with respect to resonant frequency and resonant inductor's ratio. They can be summarized as follows:

- Case 1: When switching frequency is greater than resonant frequency
 - $A > 1, (L_r > L_m)$
 - $A = 1, (L_r = L_m)$
 - $A < 1, (L_r < L_m)$
- Case 2: When switching frequency is equal to resonant frequency
 - $A > 1, (L_r > L_m)$
 - $A = 1, (L_r = L_m)$
 - $A < 1, (L_r < L_m)$
- Case 3: When switching frequency is less than resonant frequency
 - $A > 1, (L_r > L_m)$
 - $A = 1, (L_r = L_m)$
 - $A < 1, (L_r < L_m)$

The full bridge configuration of LLC SPRC resonant converter is simulated. The converter was operated for a DC input voltage of 300V for a resonant frequency of 100 kHz and a resistive load of 100 ohms for all the above cases. The best output was obtained for the case when switching frequency is equal to resonant frequency with inductor's ratio as unity. The simulation circuit for the full bridge configuration of the LLC Converter is as given in Figure 19.

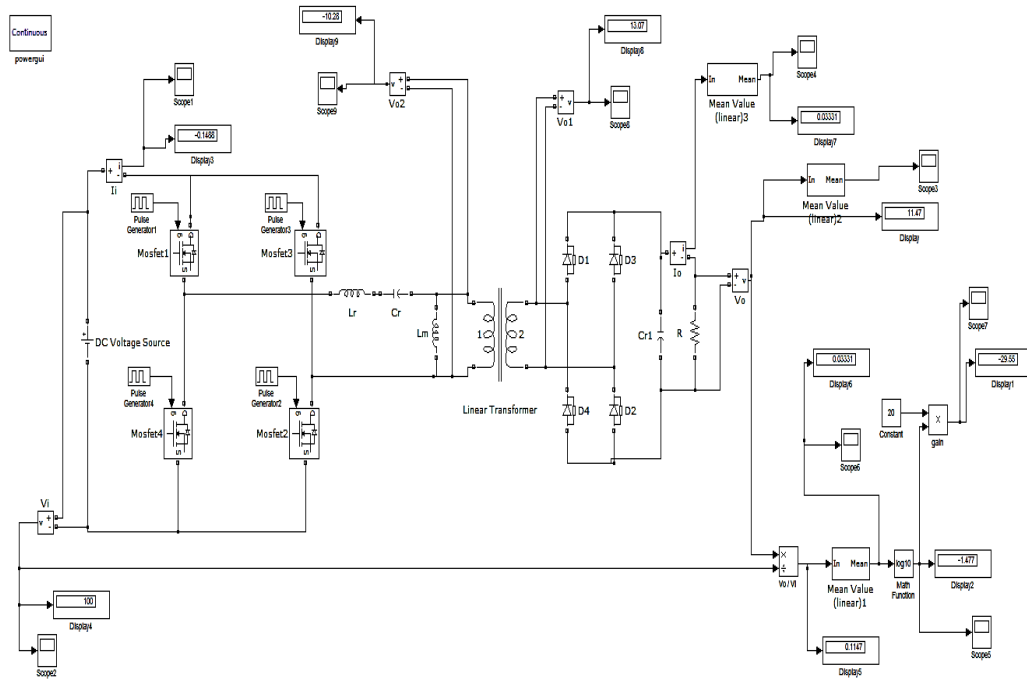


Figure 19. Simulation Circuit of LLC SPRC Resonant Converter Full Bridge Configuration

The output voltage and gain plots for the above simulation circuit have been shown in Figure 20 and in Figure 21 for the best possible case, i.e., at switching frequency equal to resonant frequency for resonant inductor ratio = 1. In the above two plots, the output voltage is approximately 55 Volts for a gain of -14.

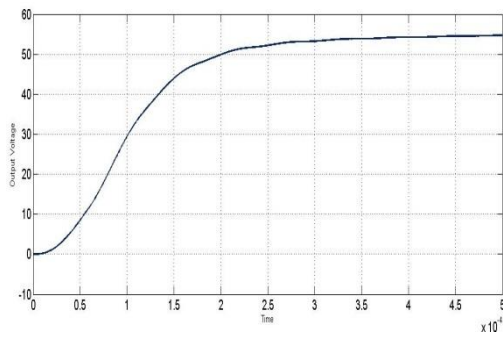


Figure 20. Output Voltage of LLC SPRC

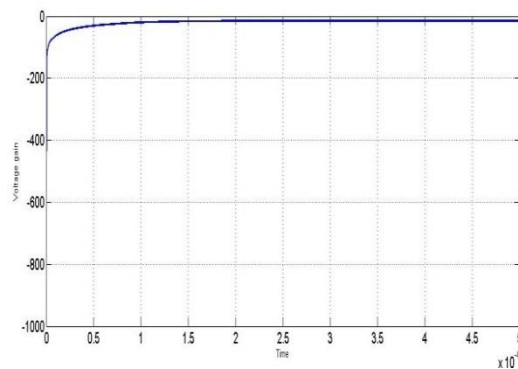


Figure 21. Output Voltage Gain of LLC SPRC

5.2. LLC-LC Resonant Converter

The parameters are kept same as that for LLC Resonant converter and the simulation is carried out for the full bridge configuration of LLC-LC converter. The simulation circuit for LLC-LC is carried out for the most efficient case and is shown in Figure 22. The plots for output voltage and the voltage gain are shown in Figure 23 and Figure 24 respectively. Output voltage for LLC-LC converter is approximately 132 Volts and the gain is found to be approximately -7.4.

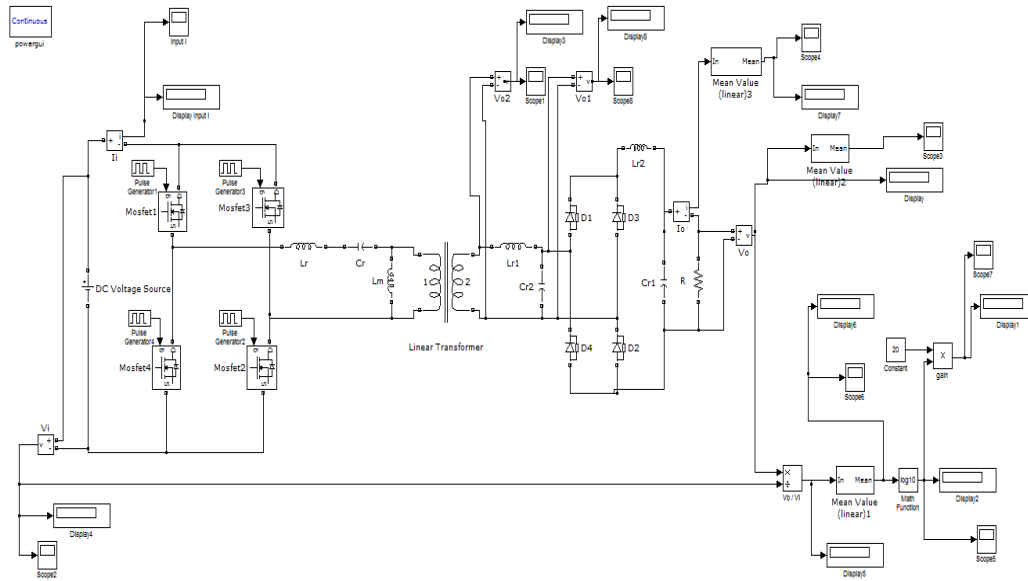


Figure 22. Simulation Circuit for LLC-LC SPRC Resonant Converter for Full Bridge Configuration

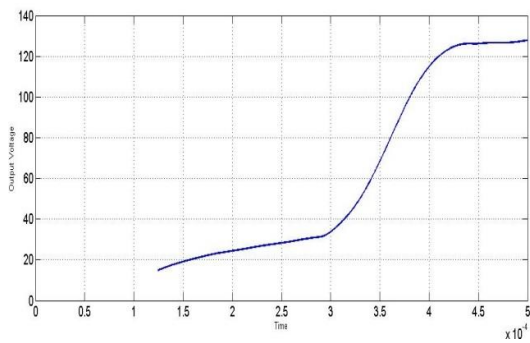


Figure 23. Output Voltage for LLC-LC SPRC

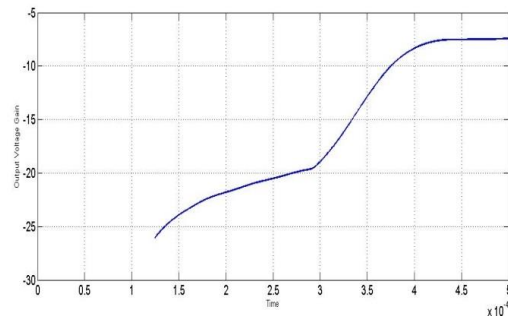


Figure 24. Output Voltage Gain for LLC-LC SPRC

5.3. LLC versus LLC-LC Resonant Converter

As seen from the outputs for both the configuration, it is found that the output voltage for LLC-LC configuration is found to be approximately more than twice to that of LLC configuration. The gain is also increased. But it is observed that LLC-LC takes more time to stabilize in comparison to the LLC converter. The simulation is carried out for three different input voltages for the same set of parameters under the condition so as to obtain the maximum efficiency. The performance analyses of both, LLC & LLC-LC are enlisted in the form of Table 1 and Table 2. Eventually it is observed that the efficiency increases with increasing input voltage and is found to be more for LLC-LC rather than LLC configuration.

Table 1.LLC SPRC Resonant Converter

S. No.	Input Voltage(V)	Output Voltage(V)	Gain	Efficiency (%)
1.	100	18.18	-14.89	48.09
2.	200	36.69	-14.81	50.42
3.	300	55.24	-14.78	51.39

Table 2. LLC-LC Resonant Converter

S. No.	Input Voltage(V)	Output Voltage(V)	Gain	Efficiency (%)
1.	100	41.5	-9.032	49.52
2.	200	56	-10.96	54.01
3.	300	132	-7.411	55.52

5.4. Speed Control of BLDC Motor fed from LLC topology of Resonant Converter

The simulation circuit for the open loop speed control of a BLDC motor fed from LLC converter's full bridge configuration is as shown in Figure 25. The converter is contained in the resonant circuit block and the control is carried out by the pulse generated from the PWM generator.

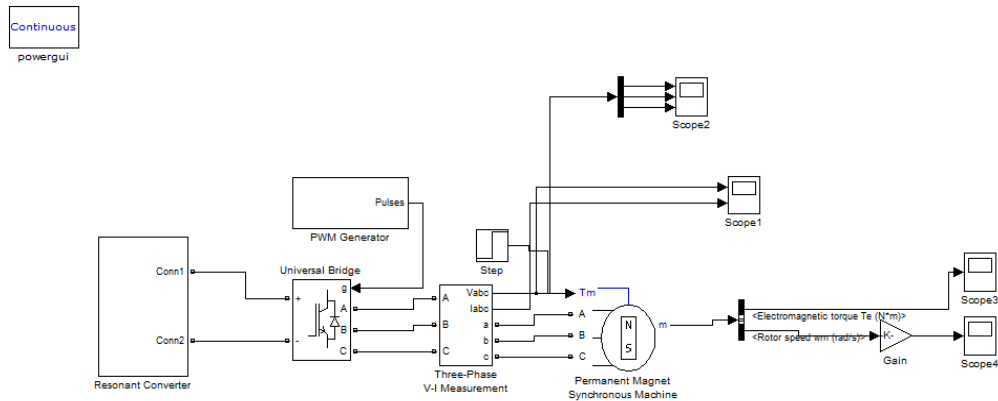


Figure 25. Simulation Circuit of Open Loop Speed Control of BLDC Motor fed from LLC Converter

The simulation results for electromagnetic torque, motor speed, output voltage and current are shown in Figure 25 to Figure 27. It is observed that open loop control is not that efficient method of speed control as it is not accurate and also the speed is also in an undesirable range.

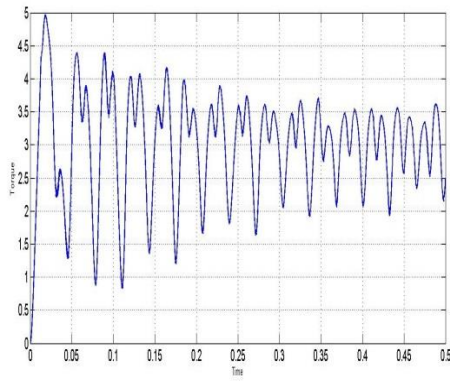


Figure 25. Torque with LLC (Open Loop)

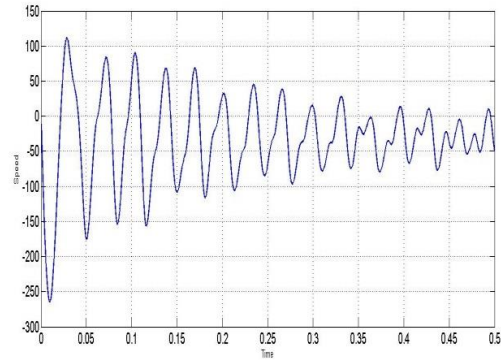


Figure 26. Speed with LLC (Open Loop)

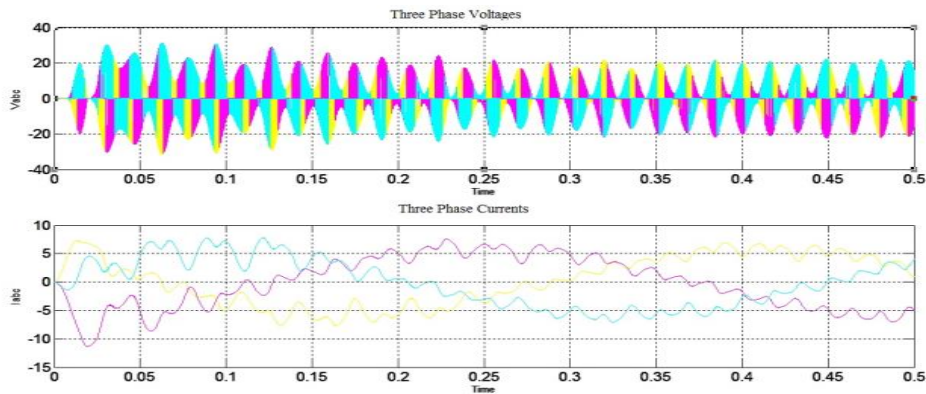


Figure 27. Three Phase Output Voltage and Current with LLC (Open Loop)

The simulation of the closed loop control of BLDC Motor fed from LLC resonant converter is as shown in Figure 28. Figure 29 to Figure 34 shows the internal building blocks of Figure 28.

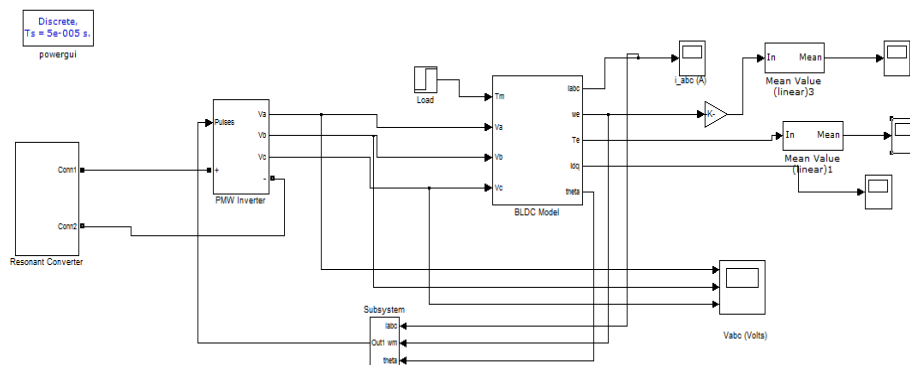


Figure 28. Simulation of Closed Loop Control of BLDC Motor Fed from LLC Converter

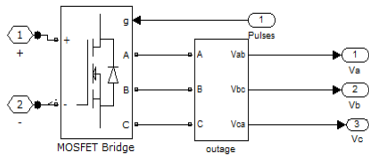


Figure 29. PWM Inverter

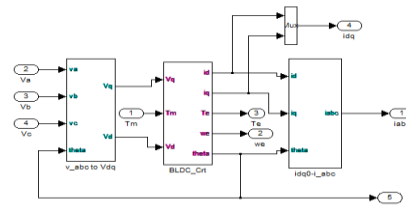


Figure 30. BLDC Motor Block

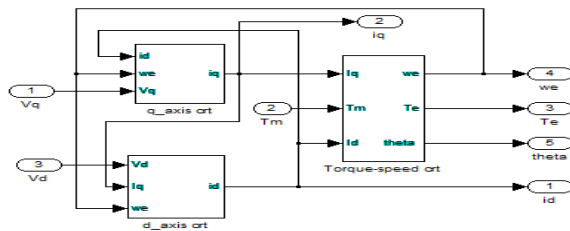


Figure 31. BLDC Control Block

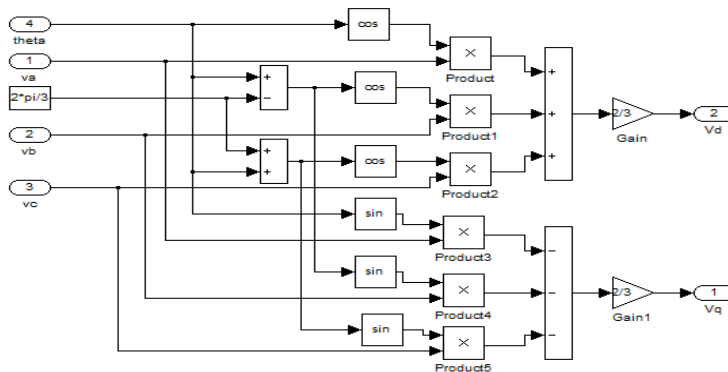


Figure 32 Vabc to Vdq Conversion Block of Figure 28. 5.13

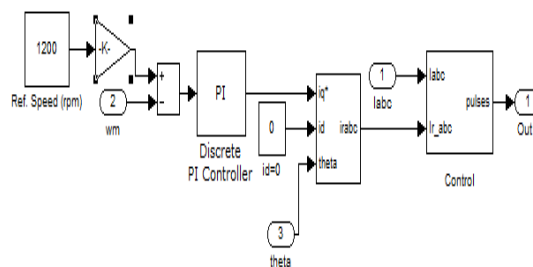


Figure 33. PI Control Circuit of the speed Subsystem Block of Figure 28

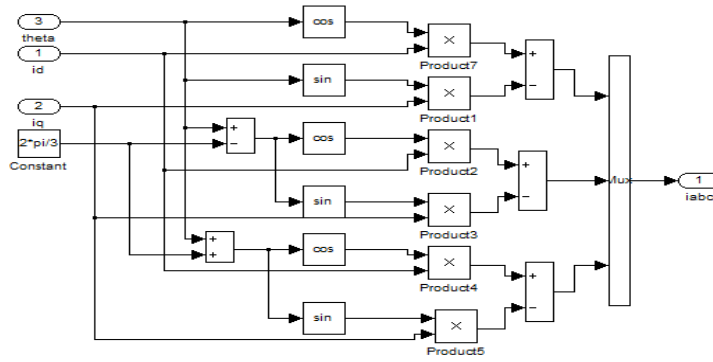


Figure 34. I_{dq} to I_{abc} Conversion Block of Figure 31

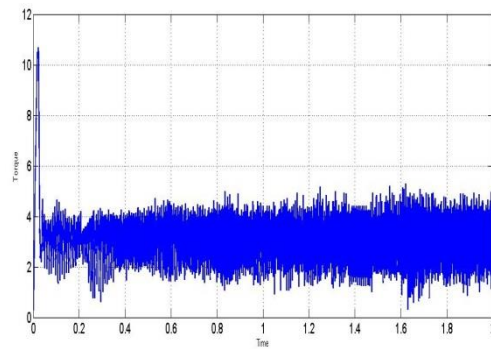


Figure 35. Torque of Closed Loop Speed Control of BLDC Motor Fed from LLC Resonant Converter

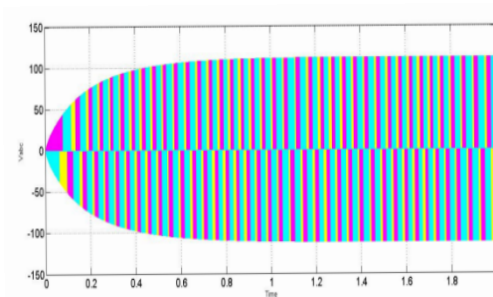


Figure 36. Speed of Closed Loop Speed Control of BLDC Motor fed from LLC Resonant Converter

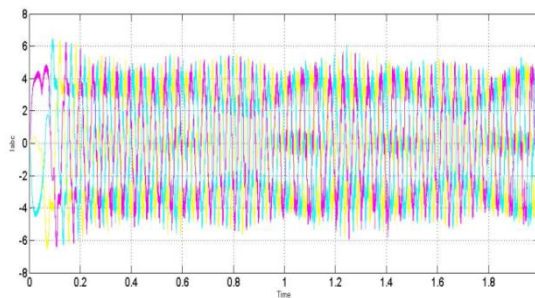


Figure 37. Output Voltage of Closed Loop Speed Control of BLDC Motor fed from LLC Resonant Converter

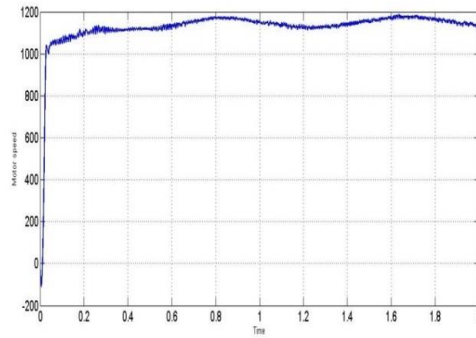


Figure 38. Output Current of Closed Loop Speed Control of BLDC Motor fed from LLC Resonant Converter

The simulation results for torque, speed, output voltage and output currents of the closed loop controlled BLDC motor fed from LLC converter is shown in Figure 35 to Figure 38.

5.5 Speed Control of BLDC Motor fed from LLC-LC topology of Resonant Converter

The simulation circuit is same as that of LLC fed BLDC Motor control, the difference only lies in the resonant converter block which in this case is designed as LLC-LC configuration. For better understanding of the performance same parameters set is considered. Since open loop control is not that efficient for this case, only closed loop control of BLDC motor fed from LLC-LC Converter is considered.

The simulation circuit is as shown in Figure 39. The output torque, speed, output three phase voltages and currents for closed loop control of BLDC motor fed from LLC-LC resonant converter are as shown in Figure 40 to Figure 43.

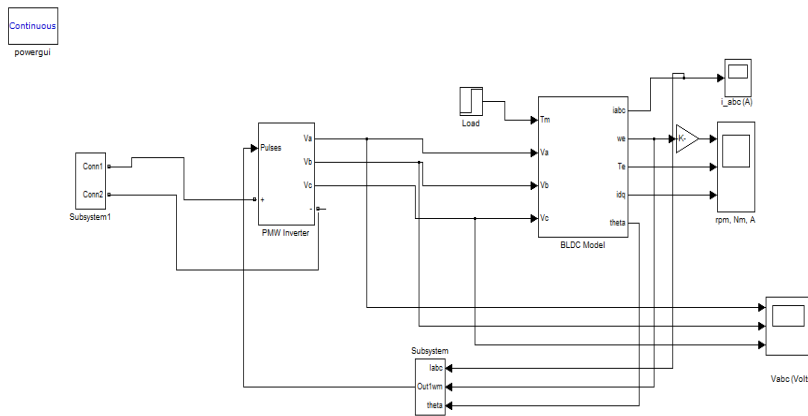


Figure 39. Simulation Circuit of Closed Loop Control of BLDC motor fed from LLC-LC Converter

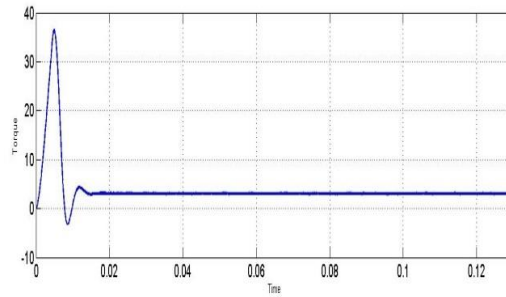


Figure 40. Torque of Closed Loop Speed Control of BLDC Motor fed from LLC-LC Converter

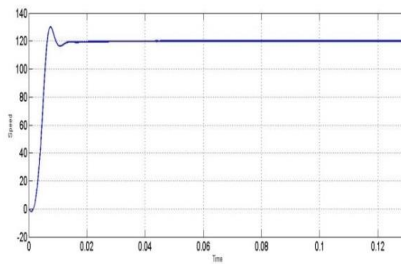


Figure 41. Speed of Closed Loop Speed Control of BLDC fed from LLC-LC converter

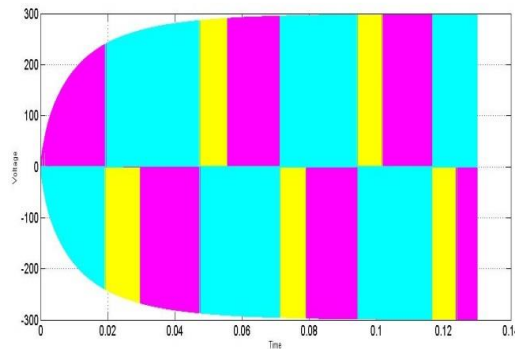


Figure 42. Output Voltage of Closed Loop Speed Control

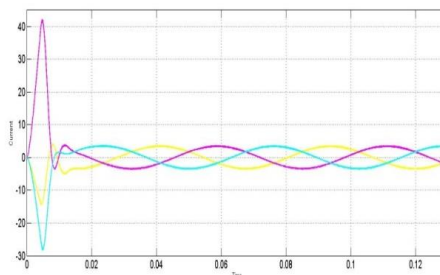


Figure 43. Output Current of Closed Loop Speed control of BLDC fed from LLC-LC Converter

6. Conclusion

The full bridge configuration for both LLC as well as LLC-LC topology were designed and their performances were analyzed based on their output voltage and voltage gain. It is observed that LLC resonant converters have some advantages when compared with other resonant converters. They are (i) LLC converters can be operated at very high frequencies owing to lossless Zero current and Zero voltage switching. The LLC converter requires only a very narrow variation of switching frequency to control the output voltage. Moreover the output voltage can be either stepped up or down while operating with wide load variation. (ii) If the transformer leakage and magnetising inductances are also considered as resonant elements while designing, the size of the other inductance can be reduced. (iii) The series capacitor blocks dc which is favourable for isolation transformer. The above features make LLC converter as a suitable choice for offline application. (iv) Highest efficiency can be achieved at high input voltage. Hence the converter can be optimised for normal operating conditions. (v) The voltage stress on the secondary rectifier diodes is reduced to two times the output voltage as there is no secondary filter inductor.

The modified LLC (LLC-LC) converter proposed in this paper has some advantages over the LLC converter. In LLC Converter, large inductance ratio and wide switching frequency variations are required to achieve wide output adjustment range and to operate at wide input voltage and load variations. Also high frequency ringing occurs at the rectifying stage. These two problems are eliminated with the use of LLC-LC converter. The secondary rectifier diodes are turned ON and OFF at zero voltage instead of zero current which occurs in LLC converter. Due to this, switching losses that occur during reverse recovery process is eliminated.

It can be concluded that LLC-LC is found to be better than LLC yielding better efficiency as well as better output voltage and gain. Even though LLC-LC is better in aspects stated above it takes more time to stabilize. The maximum efficiency is obtained for operation at switching frequency equal to resonant frequency with resonant inductor ratio as unity. It can also be inferred that the efficiency tends to increase with increase in input voltage and hence these are suitable for high input voltage operation.

Both the converters are then implemented for the closed loop speed control of BLDC motor. On comparing the responses obtained in the form of motor speed, torque and the output voltages and current, it can be concluded that LLC operates in the desired manner. On the other hand, it is observed though more stable speeds are obtained in LLC-LC, its value is very less as compared to LLC. Hence LLC-LC is better for light load and for heavier load, LLC is better.

References

- [1] M. D. Imran and K. C. Mouli, "Simulation of a Zero Voltage Switching and Zero Current Switching Interleaved Boost and Buck Converter", *International Journal of Engineering and Computer Science*, vol. 2, no. 10, (2013), pp. 2966-2974.
- [2] R. Beiranvand, M. R. Zolghadri, B. Rashidian and S. M. HosseinAlavi, "Using LLC Resonant Converter for Designing Wide Range Voltage Source", *IEEE Transactions on Industrial Electronics*, vol. 58, no. 5, (2011).
- [3] Z. J. Fang, S. X. Duan, C. S. Chen and X. Chen, "Optimal Design Method for LLC resonant Converter with Wide Range Output Voltage", *IEEE*, (2013).
- [4] R. Sudhrasan and C. Nagakota reddy, "An Enhanced ZVS & ZCS Full Bridge Converter with Resonance Circuit in The Secondary Winding for High Power Applications", *International Journal of Engineering Research and Applications (IJERA)*, vol. 3, no. 4, (2013), pp. 1996-2001.
- [5] B. Yang, "Topology Investigation for Front End DC/DC Power Conversion for Distributed Power System", PhD. Thesis of Virginia Polytechnic Institute and State University, (2003).
- [6] M. S. Rani, J. Samantaray and S. S. Dash, "Analysis Of Full Bridge Series Parallel Resonant Converter For Battery Chargers", *Advanced Materials Research*, vol. 768 (2013), pp. 388-391

- [7] G. Yang, P. Dubus and D. Sadarnac, "Analysis of the Load Sharing Characteristics of the Series-Parallel Connected Interleaved LLC Resonant Converter", IEEE, (2012).
- [8] B. C. Kim, K. B. Park and G. W. Moon, "Asymmetric PWM Control Scheme During Hold-up Time for LLC Resonant Converter", IEEE Transactions on Industrial Electronics, vol. 59, no. 7, (2012).
- [9] S. H. Cho, C. S. Kim and S. K. Han, "High Efficiency and Low Cost Tightly Regulated Dual Output LLC Resonant Converter", IEEE Transactions on Industrial Electronics, vol. 59, no. 7, (2012).
- [10] C. H. Chang, E. C. Chang and H. L. Cheng, "A High Efficiency Solar Array Simulator Implemented Resonant DC-DC Converter", IEEE Transactions on Power Electronics, vol. 28, no. 6, (2013).
- [11] R. Y. Yu, G. K. Y. Ho, B. M. H. Pong, B. W. K. Ling and J. Lam, "Computer Aided Design and Optimization of High Efficiency LLC Series Resonant Converter", IEEE Transactions on Power Electronics, vol. 27, no. 7, (2012).
- [12] R. Beiranvand, M. R. Zolghadri, B. Rashidian and S. M. H. Alavi, "Optimizing the LLC-LC Resonant Converter Topology for Wide-Output-Voltage and Wide-Output-Load Applications", IEEE Transactions on Power Electronics, vol. 26, no. 11, (2011).
- [13] H. K. S. Ransara and U. K. Madawala, "A low cost brushless DC motor drive", IEEE Conference in Industrial Electronics and Applications, (2011).
- [14] J. Zambada, "Sensorless Field Oriented Control of PMSM Motor", Micro Chip Technology Inc.
- [15] P. S. Bimbhra, "Generalized Theory of Electrical Machines", Khanna Publishers, 21st Reprint, (2012), pp. 33-55.

Authors



M.Santhosh Rani obtained her graduation in Electrical and Electronics Engineering from College of Engineering, Guindy, Anna University, Chennai, India in 1989. She obtained her M.E in Power Electronics & Drives from Anna University, Chennai in 2004. She also holds a Diploma in maintenance Management from Annamalai University, Chidambaram, India. She is a life member of Indian Society for Technical Education. Presently she is pursuing Ph.D programme at SRM University, Chennai, India. She has published papers in International Journals and conferences. Her research interests include Power Electronics and Drives, Resonant converters and Facts Controllers.



Subhransu Sekhar Dash is presently working as a Professor in the Department of Electrical and Electronics Engineering, SRM University, Chennai, India. He has completed his graduation in Electrical Engineering in the year 1994. He got his M.E. in Power Systems Engineering from University College of Engineering, Burla, Orissa, India in 1996 and obtained his Ph.D degree from College of Engineering, Guindy, Anna University, Chennai, India in the year of 2004. He was formerly a faculty member of Anna University, College of Engineering, Guindy, Chennai, India. He has published more than 50 papers in International Journal and conferences. His research areas are Modelling of FACTS Controller, Power Electronics and Drives, Power System Stability and Artificial Intelligence. He is a life member of Indian Society for Technical Education and Institution of Engineers, India.